Customized oxygenation barrels as a new strategy for controlled wine aging

Prat-García S.[1], Nevares, I.[1*]; Martínez-Martínez, V.[1]; del Alamo-Sanza, M.[2*]
[1]Department of Agroforestry Engineering and [2]Department of Analytical Chemistry, UVaMOX-Higher Tech. Col. of Agricultural Engineering, University of Valladolid, 34001 Palencia, Spain

Abstract

The process of aging red wines in barrels is a common practice that aims to improve the quality of the wine. Oxygen, together with the compounds released by the oak wood, is responsible for this improvement through interaction with the wine compounds during the process. Wood as a natural product presents a series of highly significant discontinuities in its characteristics, not only between trees of the same species, but even between different areas of the same log. It is not surprising that, despite the homogenization of the characteristics of the wood due to the number of staves in a barrel (around 30 pieces), barrels made from the same batch of wood show very different behavior when aging the same wine. This work presents the results of applying a new way of classifying wood in cooperage by means of image analysis of the staves, based on its anatomical characteristics besides grain and handling of the staves, in order to achieve the production of barrels with a desired oxygen transfer rate (OTR) potential and also with great homogeneity between manufacturing batches. The two batches of barrels built with high and low OTR proved to be very homogeneous and the oxygen dosage of the high OTR barrels was more than twice that of the low OTR barrels, which confirmed the success of the system developed.

1. Introduction

Oak barrels have been used for centuries to age quality wines (del Alamo-Sanza, 1997; Garde-Cerdán & Ancín-Azpilicueta, 2006). The wood with which the barrel is built is generally of the genus Quercus (Martínez-Gil, del Alamo-Sanza, Sánchez-Gómez, & Nevares, 2018) which is characterized by contributing volatile and hydrosoluble compounds to the wine (Pérez-Coello, Sanz, & Cabezudo, 1998; Puech, Feuillat, Mosedale, 1999), thus modifying it sensorially and chemically. The interaction of the compounds released by the wood with the wine's own compounds is governed by the presence of atmospheric oxygen, which is essential for aging and actively involved in the evolution of the wine (Moutounet, Mazauric, Saint-Pierre, & Hanocq, 1998). Oxygen entry into the barrel, which has been known for a long time (Ribereau-Gayon,

1933), is through the wood, the joints of the staves and that of the stopper (Vivas & Glories, 1997), although other authors argue that the main route of oxygen entry occurs during the filling of the barrels (Peterson, 1976), or even that the only contribution is during the degassing of the wood in the first few days after filling (Qiu, Lacampagne, Mirabel, Mietton-Peuchot, & Ghidoss, 2018). The work previously developed by the UVaMOX group demonstrated oxygen entry through the wood of the barrel, not only in the dry state, but also when it was moistened after 40 days' contact with the wine (Nevares, Crespo, González, & Alamo-Sanza, 2014; Nevares & del Alamo-Sanza, 2015; Nevares et al., 2017, 2016). The amount of oxygen that enters the barrel through the wood, once it has been soaked, has been studied using different methodologies. Recently, dissolved oxygen (DO) has been measured with the help of luminescent sensors located inside the barrel, which have allowed oxygen entry over one year to be evaluated, thus obtaining the kinetics of the annual oxygen transfer rate (OTR), defined by a decrease in the OTR with the aging time governed by the wetting of the wood(del Alamo-Sanza & Nevares, 2014; Nevares et al., 2016)

When a barrel is filled, the wood gets wet and impregnated with wine (Feuillat, 1996) which causes a decrease in the volume of wine in the barrel. If the barrel is airtight, changes occur in its shape as it tries to adapt to the new volume of liquid contained (Moutounet, Mazauric, Saint-Pierre, Micaleff, & Sarris, 1994). Infiltration of wine into the wood continues until, after approximately 82 days, the humidity front of the wood reaches the outside of the stave in contact with atmospheric air (Ruiz de Adana, López, & Sala, 2005), although evaporation begins 40 days after filling (Claire et al., 2018). All of these phenomena cause changes in the internal pressure and are common in most barrels that attain closure tightness (Peterson, 1976). The origin and morphological characteristics of the wood influence the sorption and absorption of both wine and volatile compounds retained in the wood (Coelho, Domingues, Teixeira, Oliveira, & Tavares, 2019; Sedighi-Gilani et al., 2012), and the impregnation of the stave wood modifies oxygen permeability with the time of contact with the wine (Nevares et al., 2016).

The heterogeneity of wood as a natural product produces very different barrels within the same batch and cooperage, thus requiring a wood classification system to reduce this variability and allow barrels as homogeneous as possible to be offered. Most cooperages classify wood by grain (Vivas, 1995) although there is technology for the classification of wood by non-destructive processes, such as Oakscan (Michel et al., 2011; Michel & Teissèdre, 2012), based on Near Infrared Spectroscopy (NIRS) which proposes the classification of wood according to its phenolic composition. As for oxygen, the most recent studies determining the transmission of oxygen through French oak wood have established an oxygen input of ~12.3 mg/L/year (del Alamo-Sanza, Cárcel, & Nevares, 2017). Recent work has shown that the correlation of wood grain with the rate of oxygen entry through wood, although important, is not statistically significant (Nevares

et al., 2019) requiring the use of a total of nine anatomical properties in order to explain and predict the greater or lesser oxygen permeability of *Quercus petraea* wood (Martínez-Martínez, Alamo-Sanza, & Nevares, 2019).

The objective of this work is the construction of barrels with different OTR using wood classified in a non-destructive way by image analysis for the recognition of its anatomical properties. A method was used to select the staves of each barrel seeking a customized oxygenation value and also great homogeneity between the lots of barrels built. The fabrication and evaluation of barrels using the proposed method showed that it was possible to build barrels with different rates of wine oxygenation by classifying the wood in cooperage.

2. Materials and methods

This study consisted of 4 stages. In the first place (step 1) the OTR of the staves was estimated from the physical properties of the oak boards (oak rough staves) from the cooperage wood yard, which were classified in 3 groups: high and low and the middle, in line with an OTR threshold according to their estimated OTR. The next step (2) was to select the rough staves of each previous class to build each of the barrels with a homogeneous, high or low potential wood OTR and move on to its construction. In the third stage (3) the barrels were built and finally, in the last stage (4), the real OTR of the barrels as vessels was evaluated.

2.1. Oak wood samples

For this trial, 3064 French oak (*Q. petraea*) rough staves (before bending and toasting), provided by INTONA S.L. cooperage (Navarre, Spain) as a usual batch of oak wood planks were used to construct regular barrels with a grain value between 1.88 and 4.94 mm. Oak rough stave samples were divided into two groups: 1836 oak rough staves, with a length of around 96 cm, employed to build the barrel body, and 1228 oak rough staves boards, with a length varying between 42 and 73 cm, used to build the barrel heads.

2.2. OTR estimation

2.2.1. Potential stave OTR estimation and classification

The potential OTR of the 3064 staves was estimated in the UVaMOX installations based on the density and structural features of the oak rough staves employing the previously developed method (Martínez-Martínez et al., 2019). This method employs an Artificial Neural Network to predict the potential OTR of an oak wood sample as a function of its density and seven anatomical features measured with a non-invasive procedure from an image: the rotation angle of the oak rough stave sample, the number of rings, the earlywood and latewood area ratio, and the inclination and number of medullar rays (Martínez-Martínez et al., 2019). To this end a Gibertini

CENT 4000 technical balance (Gibertini Elettronica S.R.L., Milan, Italy) combined with a 3D volumetric camera IFM O3D303 (IFM electronics, Essen, Germany) were employed to measure the weight and volume of the oak rough staves, respectively. The density was calculated by dividing the weight and volume of each rough stave. The images of the head of each stave were acquired with a JAI company GO-5000M-USB 5 MP 12-bit monochrome CMOS camera (JAI A/S, Copenhague, Denmark) with a 25 mm lens. Moreover, an IDL-W-152 LED illumination system (Infaimon S.L., Spain) was employed to illuminate the wood samples for constant and uniform illumination.

The staves´ potential OTR was estimated to classify the staves into three groups: low wood OTR (LWOTR), high wood OTR (HWOTR) and those with an estimated OTR in between according to custom threshold; they were later employed in the barrel construction stage.

2.2.2. Overall wood potential OTR estimation of barrel

Overall potential wood OTR of each barrel was calculated using the estimated OTR of the staves employed to make each barrel. The dimensions of each rough stave, which were also measured with the 3D volumetric camera to measure the volume of each rough stave in the previous subsection, had to be considered. With these data, the potential OTR of each stave was weighted by the ratio between each stave area and the total barrel area to calculate the overall wood potential OTR of the barrel.

Two assumptions about the barrel characteristics were made in order to calculate the area ratio entailed by each stave based on measurements taken in barrels disassembled from the cooperage. The first assumption was that the barrel body area was 1.50 m^2 and the second that each head barrel area was 0.25 m^2. This meant that the body was 74.77% of the total barrel area and each head area 12.61% of the total barrel area. With this in mind, the method to calculate this ratio differed depending on whether the stave formed part of the body or the head.

It is important to emphasize that the OTR estimated with this method was only the OTR of the wood staves in the barrel, which is the main pathway (up to 75% of overall OTR) of oxygen entry in French oak barrels (Nevares & del Álamo Sanza, 2014). To calculate the OTR of the barrel the oxygen that flowed between the staves also needed to be considered (Nevares et al., 2014; Qiu et al., 2018; Vivas & Glories, 1997).

2.2.2.1. Barrel body stave area

To calculate the barrel body stave's area ratio, all the stave lengths were considered to be the same. Only the width of the staves was variable, so the ratio between this and the total width of the barrel body was its percentage of the total 1.66 m^2. Equation (1) shows the ratio of each stave area.

$$ratio_i^{body} = 74.77\% \cdot \frac{w_i}{\sum_{n=1}^{N_b} w_n} \quad (1)$$

where $ratio_i^{body}$ is that of the the i-th stave of the barrel body, w_n the width of the n-th barrel body stave and N_b the number of staves of the barrel body.

2.2.2.2. Barrel head stave area

To calculate the barrel head stave area ratio their width and order of position in the barrel head had to be considered.

Figure 1.a shows an example of barrel head stave distribution. It can be seen that the width of the first and last head staves was reduced to fit into the total 0.597 m of each barrel head, which was the diameter associated with the 0.28 m^2 area of each one. With this in mind, the relation between the width measured for each stave and the equivalent width used to calculate the ratio can be seen in equations (2-4):

$$w_{1,eq}^{head} = w_1^{head} \cdot \left[1 - \frac{\left(\sum_{n=1}^{N_h} w_n^{head}\right) - 0.597}{w_1^{head} + w_{N_h}^{head}}\right] \quad (2)$$

$$w_{n,eq}^{head} = w_n^{head}, 2 \leq n \leq N_h - 1 \quad (3)$$

$$w_{N_h,eq}^{head} = w_{N_h}^{head} \cdot \left[1 - \frac{\left(\sum_{n=1}^{N_h} w_n^{head}\right) - 0.597}{w_1^{head} + w_{N_h}^{head}}\right] \quad (4)$$

where w_i^{head} and $w_{i,eq}^{head}$ are the measured and equivalent widths of the i-th stave, in meters, and N_h the number of head staves. Equations (2) and (4) reduce the width of the two extreme staves proportionally to their measured width.

Figure 1: a) Barrel head stave distribution example; b) Diagram with a generic stave, in red, in the head (in blue), with the parameters employed to calculate its area ($2 \cdot I$) in equation (5).

$$\begin{aligned} I &= \int_{x_1}^{x_2} \sqrt{R^2 - x^2} \cdot dx = \int_{x_1}^{x_2} (R^2 - x^2)^{\frac{1}{2}} \cdot dx \\ replacing &\begin{cases} x = R \cdot cos(\alpha) \\ dx = -R \cdot sen(\alpha) d\alpha \end{cases} \rightarrow \alpha = arccos\left(\frac{x}{R}\right) \\ I &= \int_{arccos\left(\frac{x_1}{R}\right)}^{arccos\left(\frac{x_2}{R}\right)} [R^2(1 - cos^2\alpha)]^{\frac{1}{2}} \cdot [-R \cdot sen(\alpha)] \cdot d\alpha = \\ &= -R^2 \cdot \int_{arccos\left(\frac{x_1}{R}\right)}^{arccos\left(\frac{x_2}{R}\right)} sen^2\alpha \cdot d\alpha \overset{*}{=} \end{aligned} \quad (5)$$

$$\overset{*}{=} \frac{-R^2}{2} \cdot \left\{ \int_{arccos\left(\frac{x_1}{R}\right)}^{arccos\left(\frac{x_2}{R}\right)} d\alpha - \int_{arccos\left(\frac{x_1}{R}\right)}^{arccos\left(\frac{x_2}{R}\right)} cos(2\alpha) \cdot d\alpha \right\} =$$

$$= \frac{-R^2}{2} \cdot \left\{ \left[arccos\left(\frac{x_2}{R}\right) - arccos\left(\frac{x_1}{R}\right) \right] - \frac{1}{2} \cdot sen(2\alpha) \Big|_{\alpha=arccos\left(\frac{x_1}{R}\right)}^{\alpha=arccos\left(\frac{x_2}{R}\right)} \right\}$$

$$I = \frac{-R^2}{2} \cdot \left\{ \left[arccos\left(\frac{x_2}{R}\right) - arccos\left(\frac{x_1}{R}\right) \right] - \frac{1}{2} \cdot \left[sen\left(2 \cdot arccos\left(\frac{x_2}{R}\right)\right) - sen\left(2 \cdot arccos\left(\frac{x_1}{R}\right)\right) \right] \right\}$$

$$* \; cos(2\alpha) = cos^2\alpha - sen^2\alpha = 1 - 2 \cdot sen^2\alpha \Rightarrow sen^2\alpha = \frac{1 - cos(2\alpha)}{2}$$

Taking the calculated equivalent width into consideration, the area associated with each stave can be calculated with the expression presented in equation (5), bearing in mind that the parameters presented in Figure 1.b. were $2 \cdot I$ as the area of the stave, R the head radius (0.2985 m), and x_1 and x_2 the position of the beginning and end of the stave, respectively. Considering the equivalent width calculated with equations (2-4) x_1 and x_2 can be worked out using the expressions presented in equations (6) and (7):

$$x_{1,i} = \begin{cases} 0 \; if \; i = 1 \\ \sum_{n=1}^{i-1} w_{n,eq}^{head} \; if \; i > 1 \end{cases} \tag{6}$$

$$x_{2,i} = x_{1,i} + w_{i,eq}^{head} \tag{7}$$

where $x_{1,i}$ and $x_{2,i}$ are the initial and final position of the i-th stave of the head, and $w_{i,eq}^{head}$ the equivalent width of the i-th stave.

Finally, considering all the previously presented equations, the ratio of a stave of the head barrel is expressed in equation (8):

$$ratio_i^{head} = 12.61\% \cdot \frac{2 \cdot I_i}{0.28} \tag{8}$$

where $ratio_i^{head}$ is the ratio of the the i-th stave of the barrel head and $2 \cdot I_i$ is the total area of the i-th stave, in m^2, calculated according to equation (5).

2.3. Stave selection and barrel construction

At the end of the previous stage, 16 packages of rough staves were obtained with the wood required to make the 16 customized oxygenation barrels and were sent to the participating cooperage for their construction. Each of the packages contained the staves making up the body, as well as the boards for the construction of the 2 heads of each barrel.

The barrels were constructed in Tonelería INTONA S.L. cooperage by experts applying the procedure employed to construct regular 225L barrels with a medium toast level. The usual dimension requirements in INTONA S.L. are a total length of 218 cm for the barrel body with at least one stave of a width wider than 10 cm in the barrel body to place the bunghole, and a set of staves for each barrel head long and wide enough to construct a circle with a radius of 29.85 cm.

In our work, other requirements related to the OTR were also considered in order to build the LWOTR and HWOTR barrels. On the one hand, the barrel head staves were randomly chosen from the LWOTR and the HWOTR stave group, respectively, taking into consideration the previously mentioned dimension requirements. On the other hand, the barrel body staves were selected from the LWOTR and HWOTR groups in order to create bodies with a similar estimated OTR. A Monte Carlo based computational method (Liu, 2008) was employed to select the barrel body staves to reduce the variability in the estimated OTR of the barrel bodies constructed.

At the end of this stage 8 high OTR wood barrels (HWOTR barrels), 8 low OTR wood barrels (LWOTR barrels) had been constructed and, in addition, the cooperage provided 4 barrels built following the usual barrel making procedure (commercial barrels). The 20 barrels were sent to UVaMOX to be studied.

2.4. Characterization of the built barrels OTR

The performance of the barrels was studied under controlled cellar conditions, with a temperature between 15-17 °C and 70-75% relative humidity. Half of the barrels built with classified wood (4 LWOTR barrels and 4 HWOTR barrels), together with two of the commercial ones built without stave classification, were used to evaluate the actual OTR. The other barrels were used to age a red wine at a later stage.

2.4.1. Follow up bung (O_2 and pressure)

The distribution of DO and barrel pressure was determined by means of a modified expandable bung, a plug that allows the passage of two optical fibers with a luminescent sensor at the end (Oxygen Dipping Probe DP-PSt6; PreSens GmbH, Germany), accurate to ±1 ppb or ±3% of the respective concentration. These probes were located at a distance of 21 and 42 cm from the bung (one third and two thirds of the total internal height of a 225L Bordeaux barrel). To facilitate the hermetic seal, the stainless steel stopper was covered with a layer of food grade silicone, which ensured an airtight seal (del Alamo-Sanza & Nevares, 2014). The oxygen probes were monitored via two OXY-4 trace v3 transmitters (PreSens GmbH, Germany), each with four channels connected to a PC, thus making simultaneous measurements at two points in the 4 barrels. The DO probes were calibrated following the manufacturer's protocol to achieve maximum performance with sodium dithionite ($Na_2S_2O_4$) at a concentration of 30 g/L in distilled water (0%

lime) and with a gaseous air-nitrogen mixture (10% air saturation, 10% lime) obtained by means of a PC-controlled gas mixer GM-3 (SensorSense, The Netherlands). Each bung had a pressure transmitter with flush membrane model S-10 calibrated from the factory -250 to 0 mbar (WIKA Alexander Wiegand SE & Co. KG, Germany) to monitor the variation of the internal pressure of each barrel.

The performance of the 10 barrels was analyzed in three successive tests: first the two commercial barrels, then the four LWOTR and finally the four HWOTR barrels.

2.4.2. Barrel preparation procedure for wood degassing measurement

Without any pre-conditioning treatment, the gaseous content of the interior of each barrel was moved with CO_2 gas with a very smooth flow and from the bottom of the barrel to move the atmospheric air from the interior avoiding mixture as much as possible, and fast enough to not affect the wood. This process was carried out until the oxygen concentration inside the barrel, measured with the previously described sensors, was less than 3.8 hPa. While supplying CO_2, the barrel was filled with a previously degassed model wine (hydroalcoholic solution at 12.4% v/v of ethanol, and pH=3.5) from the bottom of the barrel avoiding turbulence, thus displacing the CO_2 overflowing from the barrel. For de-gassing model wine to low oxygen levels, a membrane contactor, Liqui-Cel® 4×13 Extra-flow module was used (3M, Maplewood, Minesota, United States). The Liqui-Cel® module was operated in the so-called transverse-flow for the liquid, meaning that liquid flowed on the shell side of the membrane module. Inside the hollow-fiber membranes (tube or lumen side of the module) low pressure (vacuum) was maintained and nitrogen was supplied as a stripping gas working together in combo mode. Once filled the correct execution of the inert filling was confirmed with DO measurements to be always below 3.8 hPa. After this operation, the bung was closed and the monitoring and data-logging of the pressure and DO began every 10 minutes for 9 days. At the end of this period the barrels were filled with model wine to measure the volume of wine loss due to wood impregnation in this period.

2.4.3. Overall barrel OTR measurement

Once the wood degassing test of the 10 barrels full of model wine was carried out, the oxygen inlet rate in each barrel, as a container made of a permeable material, was tested in order to confirm, on the one hand, the classification methodology of the staves according to their OTR and, on the other hand, the homogeneous behavior between each of the 2 groups of customized oxygenation barrels constructed.

The barrels, as in the previous case, were filled with deoxygenated model wine and also degassed at various points inside each barrel with the help of 0.5 µm porosity sintered stainless steel micro diffusers. Nitrogen was injected at low pressure into all the barrels simultaneously thus

guaranteeing the same conditions of pressure and flow, to ensure that the concentration of DO in the interior was less than 3.8 hPa. Once this had been confirmed, the barrels were filled with oxygen-free model wine, then closed and the evolution of the DO and the internal pressure were monitored every 10 min for 10 days. As in the previous case, at the end of this period the barrels were filled with model wine to measure the volume of wine loss due to wood impregnation at this stage.

2.5. Statistical analysis

Pressure and DO data were analyzed by Microsoft Excel 2016 software.

3. Results and discussion

3.1. Rough oak wood stave characteristics

The measured characteristics of the analyzed rough oak staves are shown below. Figure 2 shows the relevant dimension of the barrel body rough staves and the head boards; barrel body length was not represented because it was constant around 96 cm for all the rough staves. It also presents the estimated OTR histogram for the barrel body staves and the head boards, respectively.

Figure 2. Relevant dimensions of the wood samples analyzed: (a) body barrel rough stave width; (b) head board width and (c) head board length. Stave potential OTR: (d) body barrel staves; (e) head board stave.

Figures 2.a-c show the variability of the oak samples considered in this work and illustrate the challenge of choosing the rough oak staves for a barrel due to its dependence on rough stave dimensions. Figures 2.d-e show the distribution of the estimated potential OTR values for the body barrel staves and the head boards. Distribution is seen to be different as they originate from two different wood populations. This meant that the samples were classified as LWOTR, mid-OTR and HWOTR separately, that is, considering different thresholds for the barrel body staves and the head boards, mainly due to the limited population of classified oak wood boards.

The number of boards used in this work determines the choice of the OTR threshold sought for each group, since we required the construction of 8 barrels of each type, meaning at least 275 boards were needed in each group. The barrel body staves were classified considering 0.554 hPa/day as the LWOTR and 1.017 hPa/day as the HWOTR thresholds in order to have 275 measured staves. The remaining staves classified as mid-OTR body staves. The barrel head boards were classified considering 0.383 hPa/day as the LWOTR threshold and 0.944 hPa/day as the HWOTR threshold in order to have 172. The remaining staves were classified as mid-OTR head staves. The number of 275 staves chosen to build the barrel bodies and 172 for the barrels heads

was decided in agreement with the cooperage workers as sufficient to build the eight barrels of each group.

3.2. Barrel construction

The barrels were constructed using the 16 packs of staves chosen in the previous stages. Table 1 presents the potential wood OTR of the different LWOTR and HWOTR barrels and allows two observations to be made. Firstly, analysis of the coefficient of variation shows that that of the barrel body (1.9% and 1.2% for the LWOTR and HWOTR barrels, respectively) was between two and three times lower than that of the heads (3.7% and 4.4% for the LWOTR and HWOTR barrels, respectively). This occurred because the head staves were randomly chosen from the LWOTR and HWOTR stave groups, while the body staves were selected using a Monte Carlo method. Secondly, the results obtained confirmed those expected in a previous study (Martínez-Martínez et al., 2019): it is possible to build a barrel with a significantly different OTR and with a small standard deviation of the barrels that belong to the LWOTR and the HWOTR groups compared with the differences among those groups. In this work, the estimated potential wood OTR of the LWOTR barrels varied between 0.37 hPa/barrel.day and 0.39 hPa/barrel.day while the estimated wood OTR of the HWOTR barrels varied from 1.23 hPa/barrel.day to 1.28 hPa/barrel.day.

Table 1: Potential wood OTR (hPa/barrel.day) of the wood of the LWOTR and the HWOTR constructed barrels, specifying also the OTR of the body and the two heads. *OTR calculated on the basis of estimated stave OTR

The barrels tested in the following section are the E, F, G, H barrels of each group, which have an average potential wood OTR of 1.24 hPa/barrel.day for the HWOTR barrels and 0.38 hPa/barrel.day for the LWOTR barrels.

3.3. OTR measurement results

3.3.1. Degassing the wood: when the wine barrels were filled, first the wood was moistened, causing the release of air that was adsorbed in the roughness of the inner side of the staves. The aim of this work was to evaluate this contribution during the first 9 days, specifically the amount of oxygen incorporated into the wine exclusively from the wood. In order to do this, the barrel was filled with an oxygen-free model wine and inerted with CO_2, i.e. as the barrel was filled, the deoxygenated liquid displaced the CO_2 (see Materials and methods).

Figure 3 shows the profiles of the increase in the DO content in the 10 barrels. The 4 LWOTR barrels show a somewhat different behavior in this process during the first four days, although most of them accumulated very similar final oxygen levels, between 26.8 and 36.6 hPa after 9 days. If we assess the oxygen accumulated in these first 9 days, in which the wood was being

wetted and therefore releasing part of the air displaced by the model wine that penetrated the wood, the velocities of oxygen incorporation into the model wine oscillated between 2.02 and 2.79 hPa/day (0.097-0.135 mg/L.day), with an average value of 2.56±0.38% hPa/day (0.124±0.018 mg/L.day). These small differences were related to the differences in behavior of the barrels' internal pressure. It was found that in barrels LWOTR-E and LWOTR-H (Figure 3.a and 3.d) the usual depression values (68-75 mbar) were reached (del Alamo-Sanza & Nevares, 2017) very quickly (in a few hours), due to rapid absorption of the wine in the wood, a phenomenon accompanied by hermetic closure which causes a very sudden descent. The joints between the barrels are unquestionably an oxygen entry point into the wine, and this is dependent on the force/pressure between the staves (Qiu, 2015). After this sudden drop in the internal pressure of the barrel, a stage of lower internal depression was observed, possibly due to the readjustments of the joints between the staves and the shape of the barrel, so it decreased smoothly over time, remaining at values of 30-40 mbar below atmospheric pressure.

On the other hand, the LWOTR-F and LWOTR-G barrels (Figure 3.b and 3.c) were not capable of maintaining the depression either because structurally they adapted perfectly to the decrease in the volume of wine caused by infiltration into the wood, or because the closure did not achieve sufficient tightness. However, these two barrels caused the wine contained to reflect a sharp increase in the concentration of DO inside, which was slowly distributed throughout the total wine volume, until its behavior was similar to the LWOTR-E and LWOTR-H barrels. Finally, the DO levels at the end of the monitoring period were very similar in the 4 LWOTR barrels.

Figure 3: Evolution of accumulated oxygen (hPa/barrel.day) and barrel internal pressure (grey color) compared to atmospheric pressure (mbar) in Low and High wood-OTR barrels during wood degassing, a) LWOTR-E, b) LWOTR-F, c) LWOTR-G, d) LWOTR-H, e) HWOTR-E, f) HWOTR-F, g) HWOTR-G, h) HWOTR-H i) Commercial E and j) Commercial F.

As for the HWOTR barrels, all of them reflected very homogeneous behavior, especially the HWOTR E, G and H barrels (Figure 3.e, 3.g and 3.h) in which the oxygen input was practically equal. The DO levels reached after 9 days were between 22.9 and 30.6 hPa per barrel (Table 2). The accumulated oxygen balance allowed us to measure the oxygen supplied to the model wine by the wood, and entry rates between 2.44 and 3.13 hPa/barrel.day (0.118-0.151 mg/L.day) were recorded with an average value of 2.91±0.33 hPa/day (0.141±0.016 mg/L.day). If the evolution of the internal pressure of the barrels is observed during the process of degassing/wetting of the wood, all of them initially suffered a very sudden drop in pressure which was maintained throughout the test with values of -35 to -50 mbar. This did not occur in the HWOTR-F barrel (Figure 3.f), which was not capable of withstanding the creation of the depression, either by adapting the volume of the barrel to the decrease in the volume of the model wine, or more

probably by a bung that was not sufficiently airtight. As a consequence of the behavior of the different internal pressures, the HWOTR-F barrel showed a slightly lower degassing than the rest of the barrels of the HWOTR group. Comparing the behavior of the high and low OTR barrels, although the wood degassing values were very similar between the LWOTR and HWOTR barrels, the latter's degassing rate was almost 14% higher than that of the LWOTR barrels.

Table 2: Oxygen release rate (hPa/barrel.day) obtained from DO measurements in barrels during the wood wetting process.

Analyzing the process of wine absorption in wood in more detail, it is important to note that the liquid absorbed in the heartwood remained mainly below the fiber saturation point (FSP), so liquid absorption by heartwood appeared to be governed by water diffusion rather than capillary flow (Johansson & Kifetew, 2010), which depends on the microstructure of hardwood (Salin, 2011). It was observed that when wood was moistened below its FSP, a swelling of the wood occured that caused dimensional change between 1% and 2%, preferably in the radial and tangential directions (del Alamo-Sanza et al., 2016; Rijsdijk & Laming, 2011). This could explain the readjustments in the shape of the barrel that gave rise to abrupt pressure variations in the first few hours (see figure 4) with the sudden rupture of the vacuum that was generated then and which caused a gradual loss of vacuum.

There was also more consistent behavior in the inner depression between the HWOTR barrels compared to the LWOTR ones (Figure 3). HWOTR barrels were capable of better maintaining the internal depression, which would show a greater structural resistance, possibly due to the fact that the wood of the HWOTR group presented morphological characteristics that would produce an advantage in this respect. On the other hand, in French oak there was a positive and significant correlation between its OTR and its proportion of earlywood (Nevares et al., 2019), which indicated that it was a more porous wood than LWOTR. Considering the losses produced in each barrel, directly related to the absorption of wine (see Table 3), the HWOTR barrels were observed to absorb a greater amount of model wine causing a greater depression inside because they withstood a greater variation in the volume of wine contained in the barrels. At the same time, this wine absorbed by the wood displaced the air contained and caused a greater accumulation of oxygen in the model wine of the HWOTR barrels. The behavior of the commercial barrels in this first wetting/degassing phase was on a par with that of the LWOTR ones.

Table 3: Variation in wood moisture from high and low OTR barrels and wine volume losses during the degassing process and OTR measurement**.**

Assuming that the supply of oxygen to the model wine during the first few days of wetting of the dry wood was due mainly to the degassing of the wood, it is important to consider the losses that measured in the barrels. In previous studies on the wetting of French oak staves in barrel situations, we found that after the first and second week of wine-to-wood contact only the 1-1.5 mm thick layer of wood had free water, which was occupying the porosity of the wood (Nevares et al., 2016). Table 3 shows the losses measured in each of the 10 barrels. It can be clearly seen that more model wine was introduced into the wood of the HWOTR barrels (62% more than in the LWOTR ones), which caused greater displacement of the air contained in the porosity of the wood and, consequently, a greater contribution of oxygen to the model wine. This was corroborated by the fact that the HWOTR barrels initially had a lower average weight than the LWOTR ones, which indicates that the wood of those barrels was somewhat less dense so the porosity of the wood was greater in the HWOTR barrels, and therefore the amount of air displaced would also be slightly greater, as can be seen in Figure 4 and Table 3.

3.3.2. Real barrel OTR measurement

After the measurements of the first initial degassing phase of the wood the rates of oxygen entry were measured in a second more stable phase, which can be assumed stationary, after the first few days of wetting. For this purpose, after completing the previous test, once the wood had been moistened in its first mm of thickness (Nevares et al., 2016), the 10 barrels filled with model wine were prepared again, as described in the Materials and methods section, to monitor the accumulation of DO.

Figure 4 shows the evolution of the accumulated DO as well as the internal pressure of all the barrels studied in this second period. In this case the LWOTR barrels behaved uniformly over the time represented and in the graphs the entry velocity can be observed in the form of a straight line with a slope ranging from 0.52 to 0.83 and representing the variation in hPa/barrel·day. The pressure variation during this process ranged from -10 to -40 mbar. The formation of this vacuum inside the barrels took place in a much more progressive way than in the previous measurement test of the initial degassing of the wood since, although the barrel was already wet, it continued to absorb model wine, causing its shape to modify and internal pressure to decrease.

Table 3 shows the quantities of model wine that had to be replaced in the barrels after this test (wine losses). It can be observed that, in general, the amount of model wine absorbed by the wood in this trial was approximately half that during the study of the degassing phase of the barrel. Bearing in mind that the barrels had been wet for about 20 days, they were below the threshold for the start of evaporation, which recent studies placed at 40 days (Claire et al., 2018), so all the losses can be considered to have contributed to the increase in wood humidity inside the barrels.

The progressive increase in wood moisture caused a decrease in the oxygen permeability of the wood, which led to a reduction in oxygen entry rates in this second trial (del Alamo-Sanza & Nevares, 2014). HWOTR barrels behaved very similarly. During the first two days the entry of oxygen followed a clearly linear trend, although from the middle of the second day all of them showed an inflection point, increasing their entry speed, which we have considered to be representative as it remained uniform during the rest of the test (see Figure 4.e, 4.g, 4.h). This behavior coincided with the stability achieved in the internal pressure of the barrels, which was generally lower than in LWOTR barrels and between -30 and -70 mbar below atmospheric pressure. Once the shape of the barrel had been structurally adapted to its new volume and there were no large variations in internal pressure, a linear oxygen input rate was observed in the four barrels studied and was relatively uniform, more so than in the case of LWOTR. Table 4 shows the oxygen input rates in this period of stationary behavior of the HWOTR barrels (CV=4.8%) and the LWOTR ones (CV=18.88%) (Table 4).

Figure 4: Evolution of accumulated oxygen and barrel internal pressure (grey color) compared to atmospheric pressure (mbar) in Low and High wood-OTR barrels after wood degassing time. The slope of the DO evolution with time is the OTR (hPa/barrel.day), where a) LWOTR-E, b) LWOTR-F, c)LWOTR-G, d) LWOTR-H, , e) HWOTR-E, f) HWOTR-F, g) HWOTR-G, h) HWOTR-H i) Commercial E and j) Commercial F.

Table 4: Oxygen transmission rates (hPa/barrel·day) for all the analyzed barrels (Low wood oxygen transfer rate barrels (LWOTR), high wood oxygen transfer rate barrels (HWOTR), commercial barrels (commercial)

Comparing the average behavior of the measurements obtained from the three groups of customized oxygenation barrels and commercial barrels, it is clear that the HWOTR barrels had a much higher oxygen input speed than the commercial ones, 69% higher, while the LWOTR barrels reached 75% of their OTR (Figure 5). Thus, and taking into consideration the limitations caused by the classification of a limited number of staves for bodies (1836 staves) and heads (1228 tables), on a daily basis barrels as high OTR containers would incorporate an average of 13.7 mg oxygen into the wine they contained, while LWOTR barrels would dose 6.1 mg, whereas commercial barrels would incorporate 8.1 mg into aging wines.

Figure 5: Average evolution of DO accumulated in the model wine of the HWOTR (n=4), LWOTR (n=4) and commercial (n=2) barrels. (standard deviation shaded and the line of regression of the measure of each type of barrel lot in black).

The results obtained from the measurements of the total real OTR of the barrels analyzed indicate that wines aged in high oxygenation barrels receive 2.3 times more oxygen than those aged in low oxygenation barrels. Estimates of the overall potential OTR of each barrel (Table 1) indicated that barrels with high oxygenation wood would theoretically provide the wine being aged with three times as much oxygen as those built with low oxygenation wood. This difference, which is statistically significant (Table 4), can be explained by the fact that the total oxygen that the wine receives when it ages in barrels is the sum of what enters through the wood and what enters through the joints between staves. In French Quercus petraea barrels, the oxygen entering through the wood can represent 75% of the total, 25% therefore being attributable to the quantity entering through the joints between staves (Nevares & del Alamo-Sanza, 2014). If these percentages are applied to the transfer rate of the commercial barrels (0.74 hPa/barrel·day) in reference to what enters through the joints between the staves, this entry route contributes 0.18 hPa/barrel·day to the wine in the barrel, a datum that could be assumed constant for the barrels manufactured in this cooperage with French oak wood. Subtracting this entry rate from the real OTR measurements recorded on the barrels, the rate of oxygen entering through the wood of the staves and that in high oxygenation barrels would be 0.375 hPa/barrel·day, while 1.085 hPa/barrel·day would enter high oxygenation barrels, resulting in a ratio of 2.9, very close to the 3.2 obtained theoretically (Table 1).

4. Conclusions

The implementation of a new system for predicting the potential OTR of staves, which, by means of image analysis of the staves, uses other anatomical properties besides grain, has allowed the classification of staves by their OTR. Even though wood is not the only way to get oxygen into a barrel, considering only the wood classified by its OTR for the formulation of the barrels, it is possible to build really different barrels in terms of the oxygen contributed to the wine they contain. Selecting the rough staves for each barrel based on homogeneity between batches, allowed two batches of barrels of a homogeneous global OTR to be constructed. The analysis of the barrels obtained confirmed that it is possible to build HWOTR barrels that will dose the wine more than twice as much as LWOTR ones, in accordance with our initial aim.

The methodology employed would allow cooperages to build customized oxygenation barrels as long as a sufficient number of staves classified by their OTR were available.

Acknowledgements

The authors express great appreciation to Tonelería INTONA (Navarre, Spain) for their collaboration. S.P.G. and V.M.M. thank IBERPHENOL for their contracts. The authors thank Ann Holliday for her services in revising the English. The work was funded by Junta de Castilla

y León VA028U16, MINECO AGL2014-54602-P and FEDER, Interreg España-Portugal Programme (Iberphenol).

References

Roussey, C., Teissier du Cross, R.., Colin, J., Raffenaud J.-C., Casalinho, J., Renouf, V., Perre, P. (2018). Study, in real-life conditions, of liquid and oxygen transfers through a barrel when aging a wine in a cellar. In *Macrowine 28-31 may 2018,* Zaragoza, Spain. Retrieved from http://www.macrowine2018.com/uploads/docs/P-117.pdf

Coelho, E., Domingues, L., Teixeira, J. A., Oliveira, J. M., & Tavares, T. (2019). Understanding wine sorption by oak wood: Modeling of wine uptake and characterization of volatile compounds retention. *Food Research International*, *116*, 249–257.

del Alamo-Sanza, M., (1997). *Envejecimiento en barricas de roble del vino tinto de la D.O. Ribera del Duero. Estudio de la evolución de los monosacáridos y de sus relaciones con los compuestos fenólicos y los porcentajes de color* (Doctoral dessertation). Analytical Chemistry, Universidad de Valladolid, Valladolid, Spain.

del Alamo-Sanza, M., Cárcel, L. M., & Nevares, I. (2017). Characterization of the Oxygen Transmission Rate of Oak Wood Species Used in Cooperage. *Journal of Agricultural and Food Chemistry*, *65*(3), 648–655.

del Alamo-Sanza, M., & Nevares, I. (2017). Oak wine barrel as an active vessel: A critical review of past and current knowledge. *Critical Reviews in Food Science and Nutrition*, *58*(16), 2711–2726.

del Alamo-Sanza, M., & Nevares, I. (2014). Recent Advances in the Evaluation of the Oxygen Transfer Rate in Oak Barrels. *Journal of Agricultural and Food Chemistry*, *62*(35), 8892–8899.

del Alamo-Sanza, M., Nevares, I., Mayr, T., Baro, J. A., Martínez-Martínez, V., & Ehgartner, J. (2016). Analysis of the role of wood anatomy on oxygen diffusivity in barrel staves using luminescent imaging. *Sensors and Actuators B: Chemical*, *237*, 1035–1043.

Feuillat, F. (1996). Contribution à l'étude des phénomènes d'échanges bois/vin/atmosphère à l'aide d'un "fût" modèle. Relations avec l'anatomie du bois de chêne (*Quercus robur* L., *Quercus petraea* Liebl.) (Doctoral dessertation) *Lab. de Recherches En Sciences Forestières de l'ENGREF*. Ecole Nationale du Génie Rural des Eaux et des Forêts, Nancy; France.

Garde-Cerdán, T., & Ancín-Azpilicueta, C. (2006). Review of quality factors on wine ageing in

oak barrels. *Trends in Food Science & Technology*, *17*(8), 438–447.

Johansson, J., & Kifetew, G. (2010). CT-scanning and modelling of the capillary water uptake in aspen, oak and pine. *European Journal of Wood and Wood Products*, *68*(1), 77–85.

Liu, J. S. (2008). *Monte Carlo Strategies in Scientific Computing*. *Springer Series in Statistics*.

Martínez-Gil, A., del Alamo-Sanza, M., Sánchez-Gómez, R., & Nevares, I. (2018). Different Woods in Cooperage for Oenology: A Review. *Beverages*, *4*(4), 94.

Martínez-Martínez, V., Alamo-Sanza, M. del, & Nevares, I. (2019). Application of image analysis and artificial neural networks to the prediction in-line of OTR in oak wood planks for cooperage. *Materials & Design*, *181*, 107979.

Michel, J., Jourdes, M., Silva, M. A., Giordanengo, T., Mourey, N., & Teissedre, P. L. (2011). Impact of concentration of ellagitannins in oak wood on their levels and organoleptic influence in red wine. *Journal of Agricultural and Food Chemistry*, *59*(10), 5677–5683.

Michel, J., & Teissèdre, P.-L. (2012). *Classification et influences des polyphénols du bois de chêne sur la qualité sensorielle des vins (Application du procédé OakScan®) (Doctoral dessertation). Universite Bordeaux, France*.

Moutounet, M., Mazauric, J. P., Saint-Pierre, B., & Hanocq, J. F. (1998). Gaseous exchange in wines stored in barrels. *Journal Des Sciences et Techniques de La Tonnellerie*, *4*, 131–145.

Moutounet, M., Mazauric, J. P., Saint-Pierre, B., Micaleff, J. P., & Sarris, J. (1994). Causes et conséquences de microdèformations des barriques au cours de l'élevage des vins. *Revue Des Oenologues*, (74), 34–39.

Nevares Domínguez, I., & del Álamo Sanza, M. (2014). Oxygène et barriques: Actualisation des connaissances Quantité et voies de pénétration de l'oxygène dans la barrique. *Revue des oenologues et des techniques vitivinicoles et oenologicques*, *41*(153), 41–44.

Nevares, I., Crespo, R., González, C., & del Alamo-Sanza, M. (2014). Imaging of oxygen permeation in the oak wood of wine barrels using optical sensors and a colour camera. *Australian Journal of Grape and Wine Research*, *20*(3), 353–360.

Nevares, I., & del Alamo-Sanza, M. (2015). Oak Stave Oxygen Permeation: A New Tool To Make Barrels with Different Wine Oxygenation Potentials. *Journal of Agricultural and Food Chemistry*, *63*(4), 1268–1275.

Nevares, I., del Alamo-Sanza, M., Martínez-Martínez, V., Menéndez-Miguélez, M., Van den Bulcke, J., & Van Acker, J. (2019). Influence of Quercus petraea Liebl. wood structure on

the permeation of oxygen through wine barrel staves. *Wood Research and Technology. Holzforschung*, *73*(9), 859–870.

Nevares, I., Martínez-Martínez, V., Martínez-Gil, A., Martín, R., Laurie, V.F., & del Álamo-Sanza, M. (2017). On-line monitoring of oxygen as a method to qualify the oxygen consumption rate of wines. *Food Chemistry*, *229*, 588–596.

Nevares, I., Mayr, T., Baro, J. A., Ehgartner, J., Crespo, R., & del Alamo-Sanza, M. (2016). Ratiometric Oxygen Imaging to Predict Oxygen Diffusivity in Oak Wood During Red Wine Barrel Aging. *Food and Bioprocess Technology*, *9*(6), 1049–1059.

Pérez-Coello, M. S., Sanz, J., & Cabezudo, M. D. (1998). Gas chromatographic-mass spectrometric analysis of volatile compounds in oak wood used for ageing of wines and spirits. *Chromatographia*, *47*(7–8), 427–432.

Peterson, R. G. (1976). Formation of Reduced Pressure in Barrels During Wine Aging. *American Journal of Enology and Viticulture*, *27*(2), 80–81.

Puech, J.-l., Feuillat, F., Mosedale, J. R. (1999). The tannins of oak heartwood: Structure, properties, and their influence on wine flavor. *American Journal of Enology and Viticulture*, *50*(4), 469–478.

Qiu, Y. (2015). *Phénomènes de transfert d'oxygène à travers la barrique (Doctoral dessertation)*. Sciences agricoles. Université de Bordeaux, France. Retrieved from https://tel.archives-ouvertes.fr/tel-01340867/document

Qiu, Y., Lacampagne, S., Mirabel, M., Mietton-Peuchot, M., & Ghidoss, R. (2018). Oxygen desorption and oxygen transfer through oak staves and oak stave gaps: an innovative permeameter. *OENO One*, *52*(1), 1–14.

Ribereau-Gayon, J. (1933). *Contribution à l'étude des oxydations et réductions dans les vins (Doctoral dessertation)*. Université de Bordeaux, Bordeaux, France.

Rijsdijk, Jan .F. & Laming, Peter B. (2011). *Physical and Related Properties of 145 Timbers: Information for practice*. London: Dordrecht: Springer.

Ruiz de Adana, M., López, L. M., & Sala, J. M. (2005). A Fickian model for calculating wine losses from oak casks depending on conditions in ageing facilities. *Applied Thermal Engineering*, *25*(5–6), 709–718.

Salin, J.-G. (2011). Fibre level modelling of free water behaviour during wood drying and wetting. *Maderas. Ciencia y Tecnología*, *13*(2), 153–162.

Sedighi-Gilani, M., Griffa, M., Mannes, D., Lehmann, E., Carmeliet, J., & Derome, D. (2012).

Visualization and quantification of liquid water transport in softwood by means of neutron radiography. *International Journal of Heat and Mass Transfer*, *55*(21–22), 6211–6221.

Vivas, N. (1995). The notion of grain in cooperage. *Journal Des Sciences et Techniques de La Tonnellerie*, *1*, 17–32.

Vivas, N., & Glories, Y. (1997). Modélisation et calcul du bilan des apports d'oxygène au cours de l'élevage des vins rouges. II. Les apports liés au passage d'oxygène au travers de la barrique. *Progrès Agricole et Viticole*, *114*(13–14), 315–316.

Table 1: Potential wood OTR (hPa/barrel.day) of the wood of the HWOTR and the LWOTR constructed barrels, specifying also the OTR of the body and the two heads. [1]OTR calculated on the basis of estimated stave OTR

Barrel type	Barrel reference	Body OTR	1st head OTR	2nd head OTR	Barrel OTR[1]
High wood OTR barrels	H-A	1.254	1.145	1.222	1.236
	H-B	1.291	1.227	1.284	1.282
	H-C	1.251	1.226	1.253	1.248
	H-D	1.262	1.153	1.189	1.239
	H-E	1.238	1.199	1.199	1.228
	H-F	1.262	1.121	1.165	1.232
	H-G	1.271	1.172	1.172	1.246
	H-H	1.278	1.129	1.225	1.252
mean		*1.263 a*	*1.192 a*		*1.245 a*
min		*1.238*	*1.121*		*1.228*
max		*1.291*	*1.284*		*1.282*
SD		*0.016*	*0.044*		*0.016*
%VC		*1.2*	*3.7*		*1.3*
Low wood OTR barrels	L-A	0.398	0.33	0.373	0.386
	L-B	0.392	0.363	0.366	0.385
	L-C	0.398	0.354	0.365	0.388
	L-D	0.396	0.352	0.372	0.388
	L-E	0.397	0.356	0.356	0.387
	L-F	0.403	0.319	0.344	0.385
	L-G	0.376	0.345	0.373	0.372
	L-H	0.396	0.373	0.373	0.39
mean		*0.394 b*	*0.357 b*		*0.385 b*
min		*0.376*	*0.319*		*0.372*
max		*0.403*	*0.373*		*0.39*
SD		*0.007*	*0.016*		*0.005*
%VC		*1.9*	*4.4*		*1.4*
p level		***	***		***

*mean, minimum (min) and maximum (max) values, standard deviation (SD), and variation coefficient (%VC), *** $p<0.001$*

Table 2: Oxygen release rate (hPa/barrel.day) obtained from DO measurements in barrels during the wood wetting process.

High wood OTR barrels				Low wood OTR barrels				Commercial barrels		*p level*
E	F	G	E	E	F	G	H	E	F	
3.13	2.44	3.12	2.72	2.86	2.02	2.79	2.59	2.72	2.32	
0.98	0.95	0.95	0.91	0.87	0.65	0.34	0.98	0.91	0.78	R^2
2.91±0.32*				2.56±0.38*				2.52±0.28*	2.52±0.28*	ns

**mean±SD (standard deviation), ns: no significative*

Table 3: Variation in wood moisture from high and low OTR barrels and wine volume losses during the degassing process and OTR measurement

	High wood OTR barrels							Low wood OTR barrels							Commercial barrels					*p level*
	E	F	G	H	Mean	SD		E	F	G	H	Mean	SD		E	F	Mean	SD		
initial barrel weight (kg)	49.9	49.4	50.3	50.3	49.98	0.43	a	50	50.6	49.8	50.2	50.15	0.34	a	48.2	49.1	48.65	0.64	b	*
Degassing																				
wine losses (mL)	1600	2340	1700	1550	1797.5	367.0	a	1000	1220	1440	1140	1200.0	184.0	b	2457	1950	2203.5	358.5	a	*
barrel humidity increase (%)	3.14	4.63	3.31	3.02	3.52	0.75		1.96	2.36	2.83	2.22	2.34	0.37		4.99	3.89	3.08	0.78		ns
OTR																				
wine losses (mL)	800	900	700	620	755.0	121.5		400	800	830	800	707.5	205.5		800	680	740	84.9		ns
barrel humidity increase (%)	1.57	1.78	1.36	1.21	1.48	0.25		0.78	1.55	1.63	1.56	1.38	0.40		1.62	1.36	1.13	0.64		ns

mean, standard deviation (SD), ns: no significative, (*) p<0.05;

Table 4: Oxygen transmission rates (hPa/barrel.day) for all the analyzed barrels (high wood oxygen transfer rate barrels, HWOTR, Low wood oxygen transfer rate barrels, LWOTR), commercial barrels, commercial)

	HWOTR	R^2	LWOTR	R^2	Commercial	*p level*
Barrel E	1.23	0.96	0.69	0.98	0.90	0.95
Barrel F	1.30	0.99	0.52	0.71	0.74	0.99
Barrel G	1.26	0.96	0.83	0.79		
Barrel H	1.37	0.99	0.66	0.95		
Mean±SD	1.29±0.06b		0.68±0.13a		0.82±0.11a	0.0002

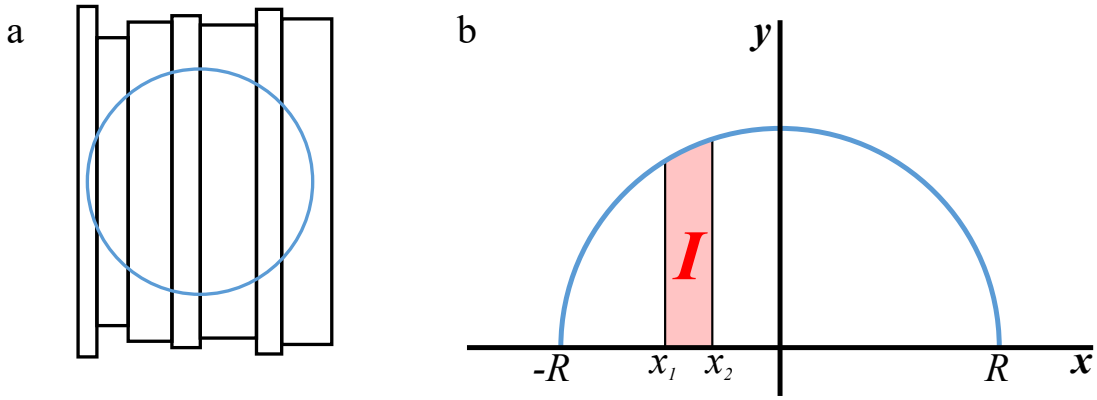

Fig. 1. (a) Barrel head stave distribution example; (b) Diagram with a generic stave, in red, in the head (in blue), with the parameters employed to calculate its area (Â) in equation (5).

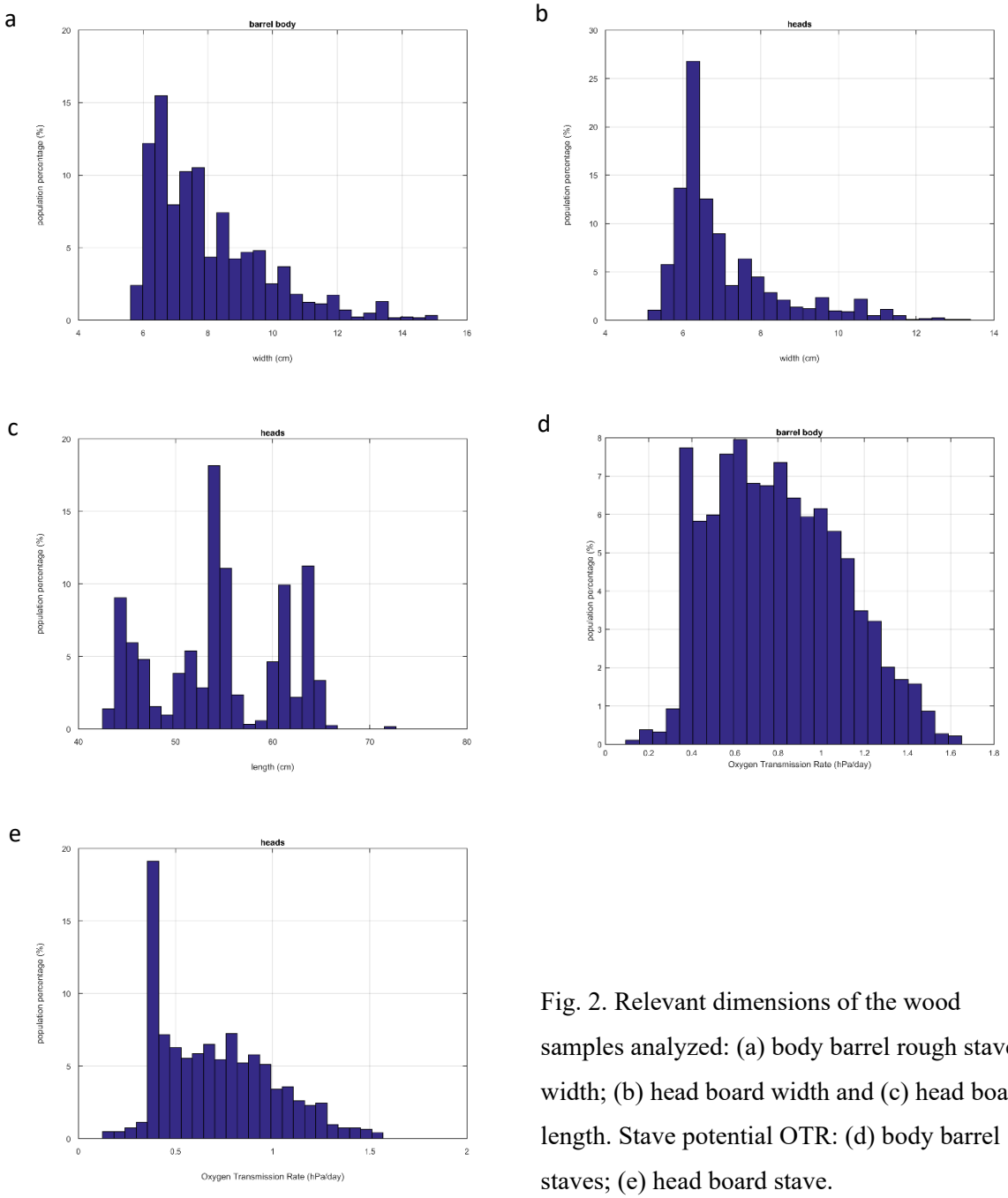

Fig. 2. Relevant dimensions of the wood samples analyzed: (a) body barrel rough stave width; (b) head board width and (c) head board length. Stave potential OTR: (d) body barrel staves; (e) head board stave.

Fig. 3. Evolution of accumulated oxygen (hPa/barrel·day) and barrel internal pressure (grey color) compared to atmospheric pressure (mbar) in Low and High wood-OTR barrels during wood degassing, (a) LWOTR-E, (b) LWOTR-F, (c) LWOTR-G, (d) LWOTR-H, (e) HWOTR-E, f) HWOTR-F, (g) HWOTR-G, (h) HWOTR-H (i) Commercial E and (j) Commercial F.

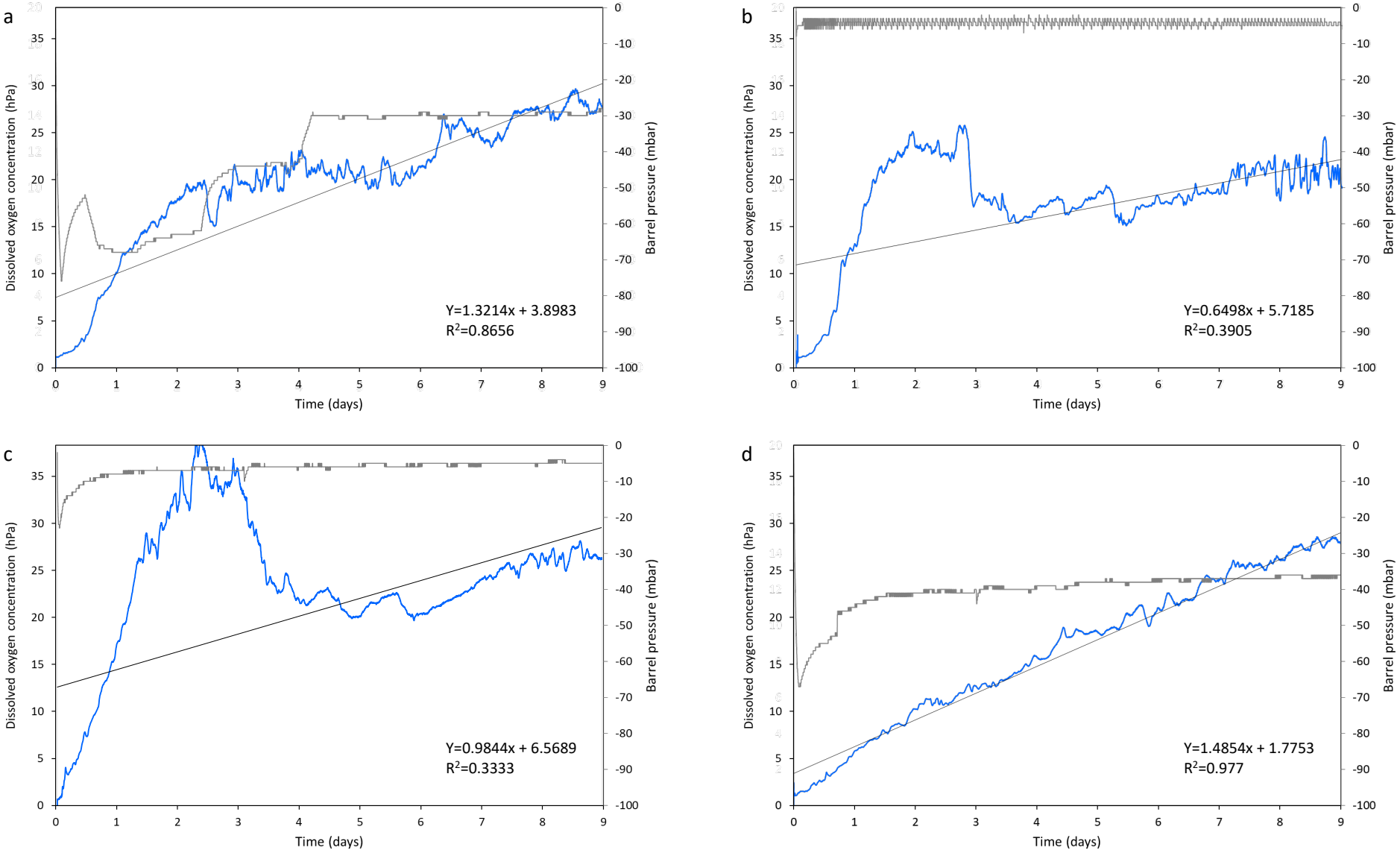

e

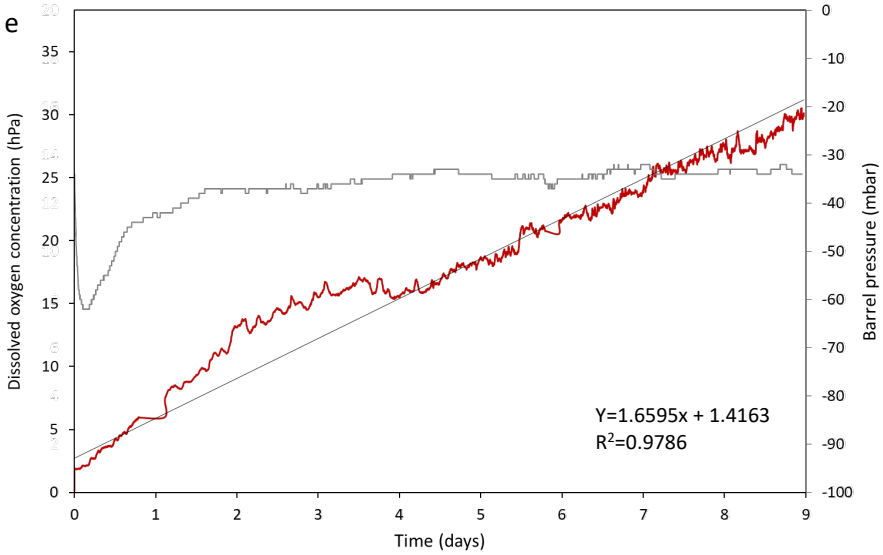
Dissolved oxygen concentration (hPa)
Barrel pressure (mbar)
Time (days)
Y=1.6595x + 1.4163
R²=0.9786

f

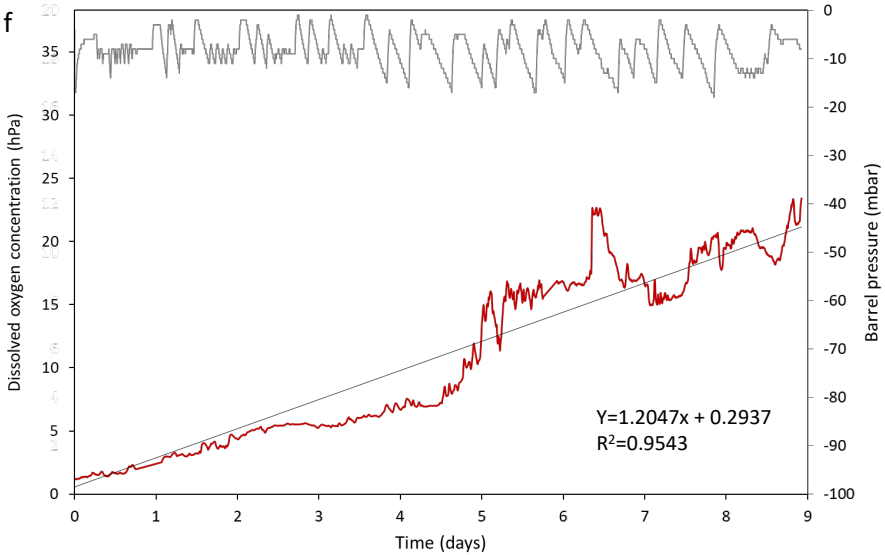
Dissolved oxygen concentration (hPa)
Barrel pressure (mbar)
Time (days)
Y=1.2047x + 0.2937
R²=0.9543

g

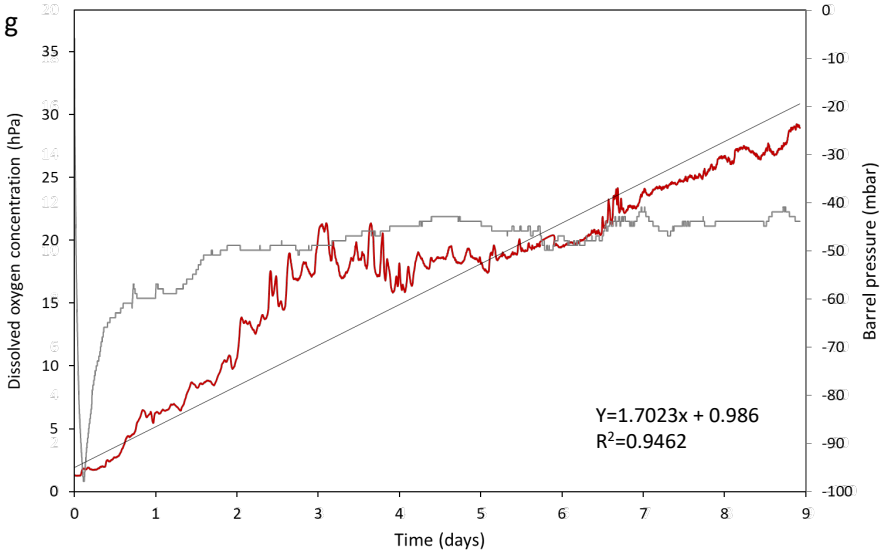
Dissolved oxygen concentration (hPa)
Barrel pressure (mbar)
Time (days)
Y=1.7023x + 0.986
R²=0.9462

h

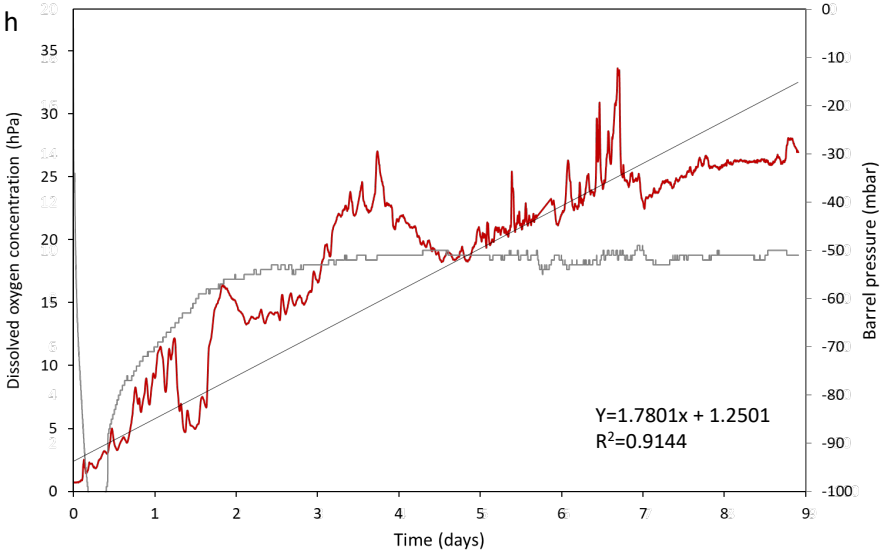
Dissolved oxygen concentration (hPa)
Barrel pressure (mbar)
Time (days)
Y=1.7801x + 1.2501
R²=0.9144

i

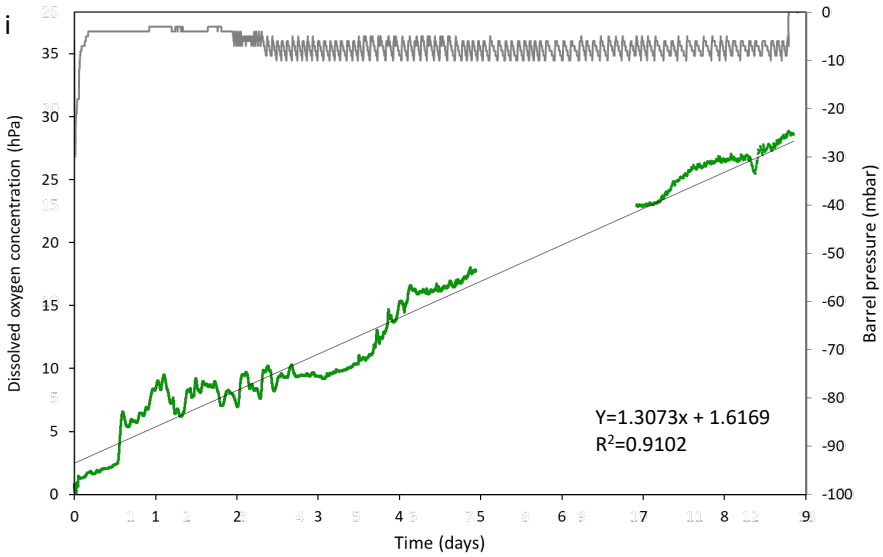
Dissolved oxygen concentration (hPa)
Barrel pressure (mbar)
Time (days)
Y=1.3073x + 1.6169
R2=0.9102

j

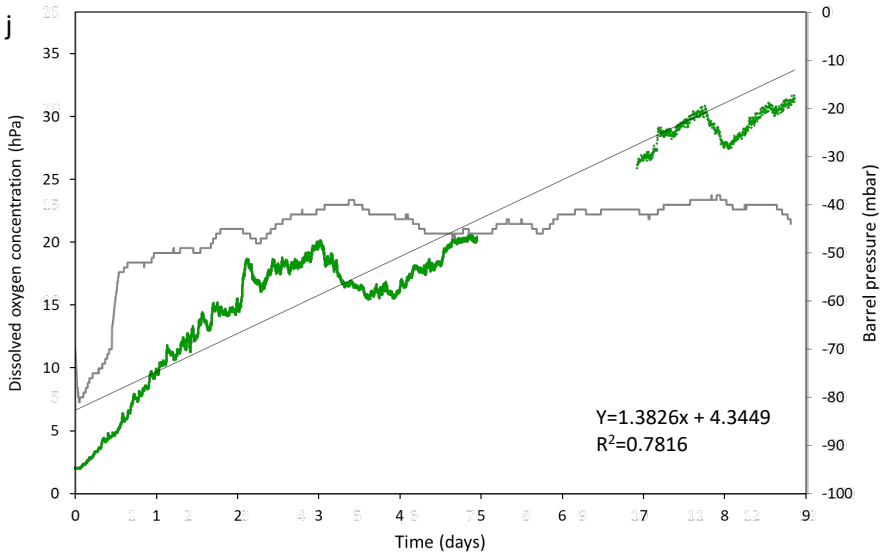
Dissolved oxygen concentration (hPa)
Barrel pressure (mbar)
Time (days)
Y=1.3826x + 4.3449
R2=0.7816

Fig. 4. Evolution of accumulated oxygen and barrel internal pressure (grey color) compared to atmospheric pressure (mbar) in Low and High wood-OTR barrels after wood degassing time. The slope of the DO evolution with time is the OTR (hPa/barrel·day), where (a) LWOTR-E, (b) LWOTR-F, (c) LWOTR-G, (d) LWOTR-H, (e) HWOTR-E, (f) HWOTR-F, (g) HWOTR-G, (h) HWOTR-H (i) Commercial E and (j) Commercial F.

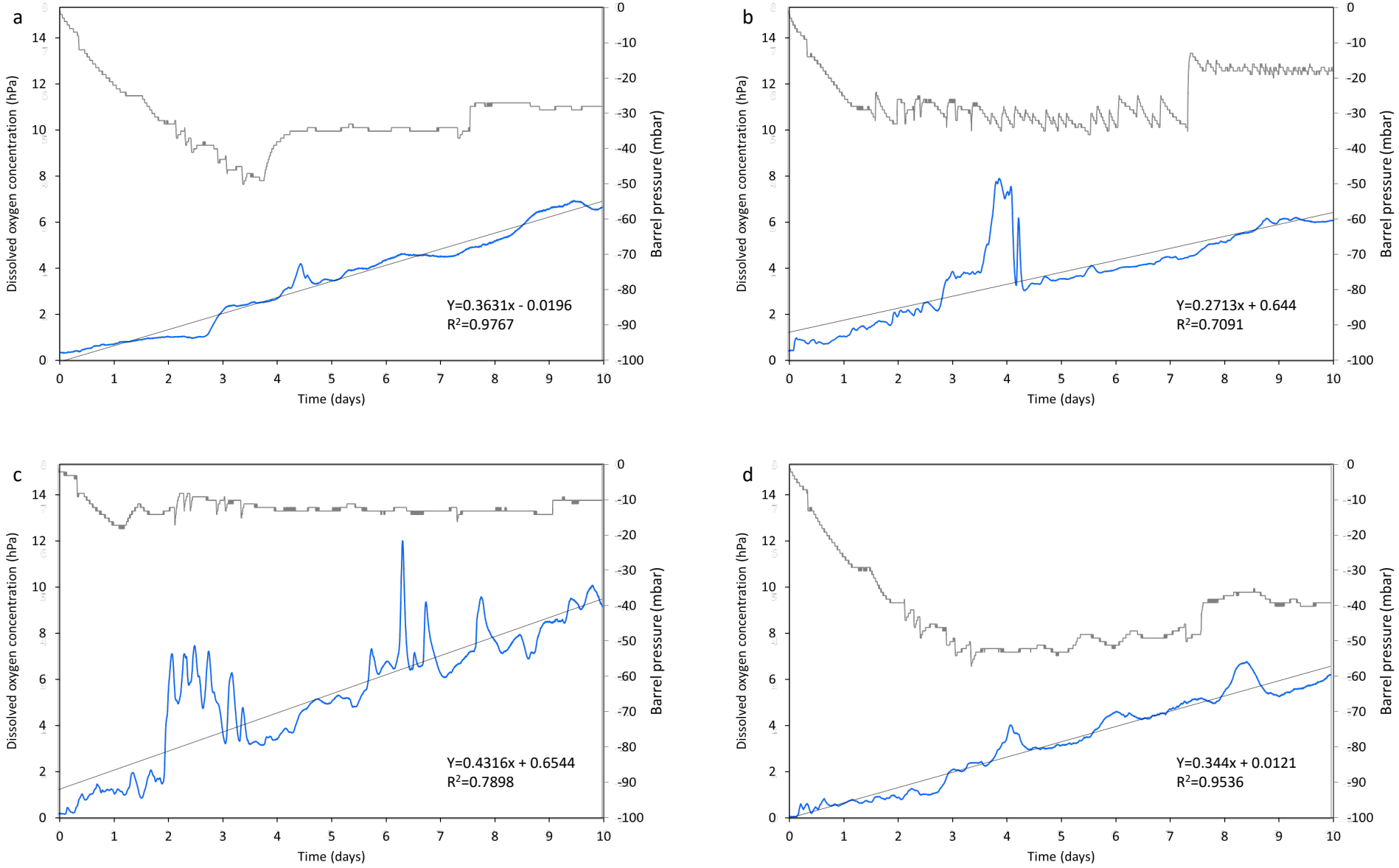

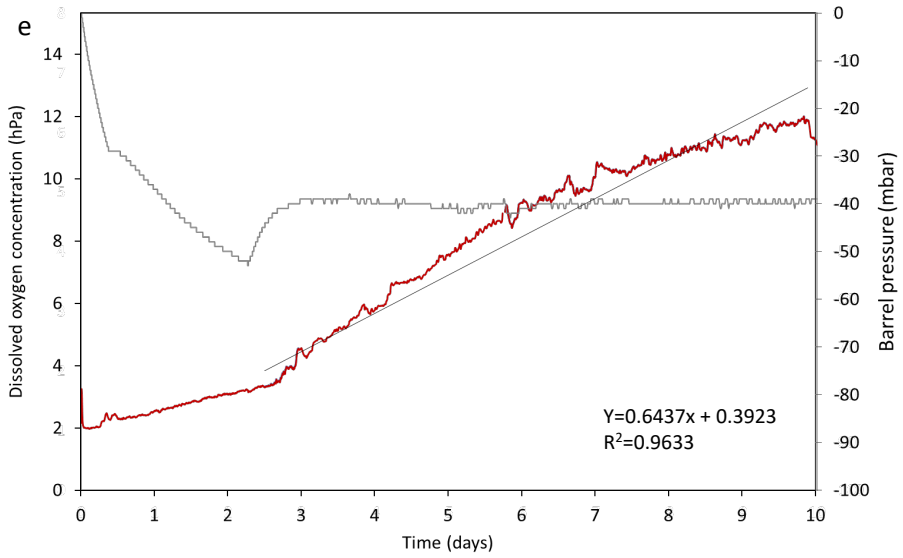
e
Dissolved oxygen concentration (hPa)
Barrel pressure (mbar)
Time (days)
Y=0.6437x + 0.3923
R²=0.9633

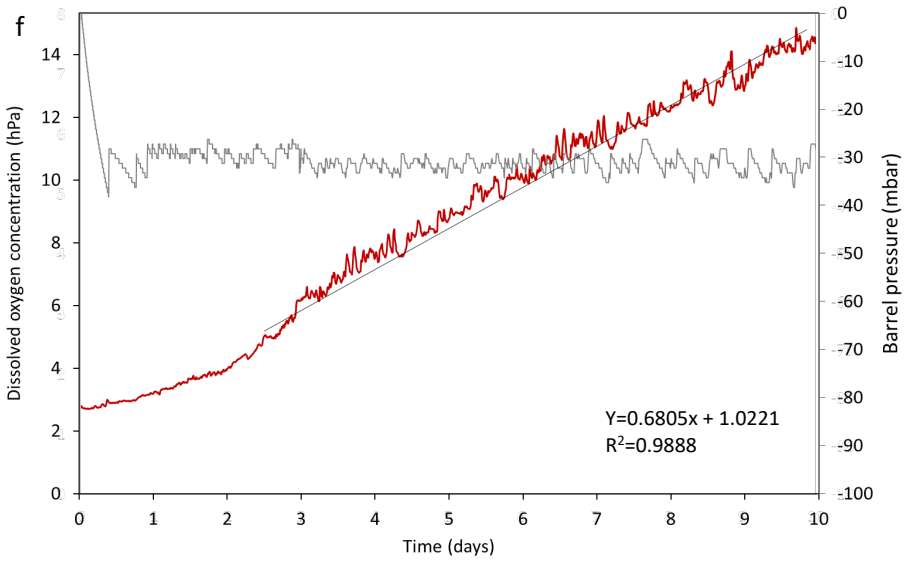
f
Dissolved oxygen concentration (hPa)
Barrel pressure (mbar)
Time (days)
Y=0.6805x + 1.0221
R²=0.9888

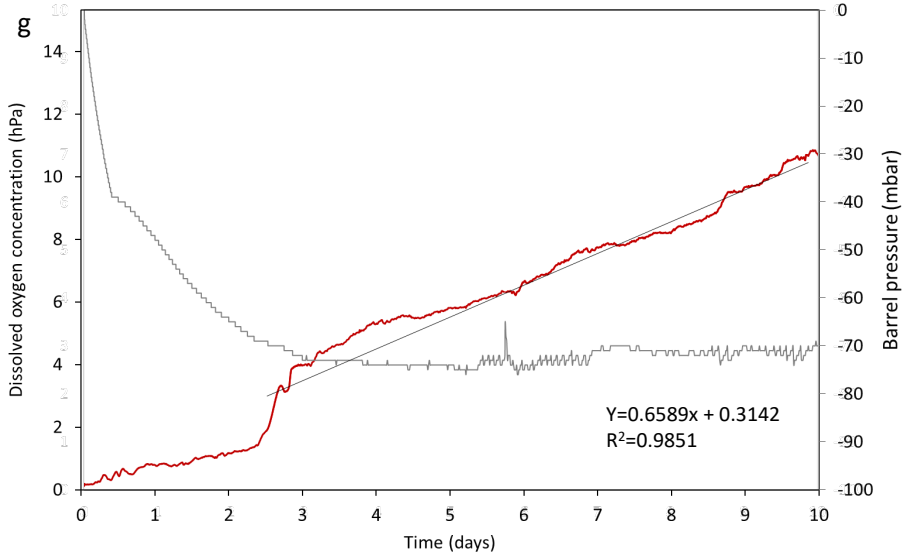
g
Dissolved oxygen concentration (hPa)
Barrel pressure (mbar)
Time (days)
Y=0.6589x + 0.3142
R²=0.9851

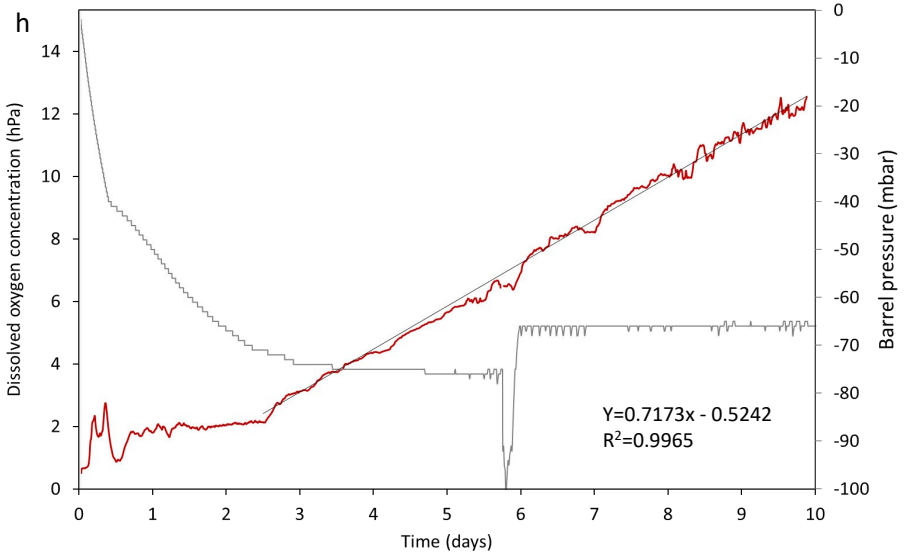
h
Dissolved oxygen concentration (hPa)
Barrel pressure (mbar)
Time (days)
Y=0.7173x - 0.5242
R²=0.9965

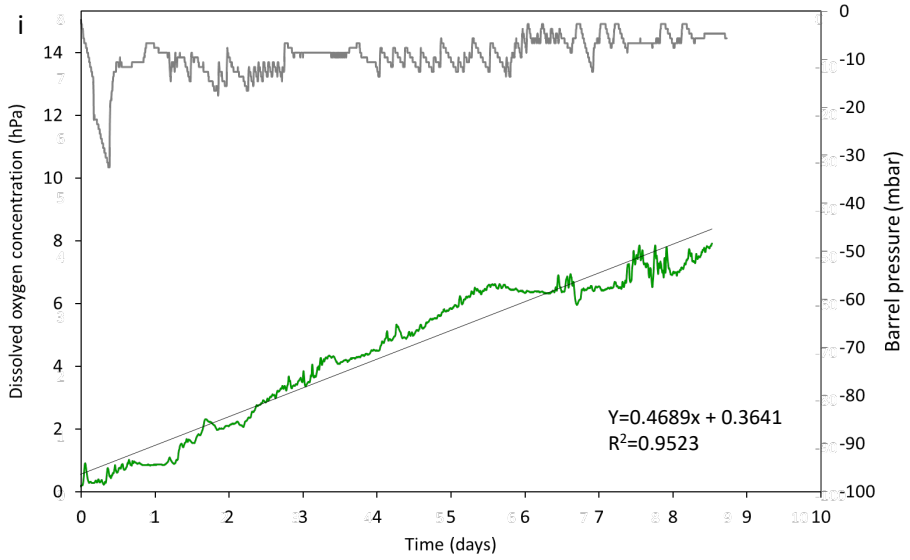
i
Dissolved oxygen concentration (hPa)
Barrel pressure (mbar)
Time (days)
Y=0.4689x + 0.3641
R²=0.9523

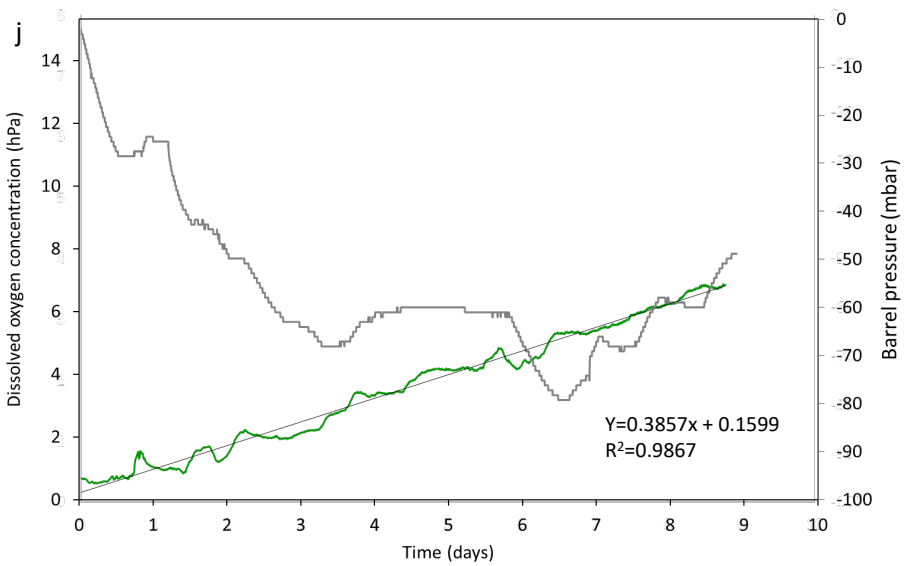
j
Dissolved oxygen concentration (hPa)
Barrel pressure (mbar)
Time (days)
Y=0.3857x + 0.1599
R²=0.9867

Fig. 5. Average evolution of DO accumulated in the model wine of the HWOTR (n=4), LWOTR (n=4) and commercial (n=2) barrels. (Standard deviation shadedand the line of regression of the measure of each type of barrel lot in black).